Modulation-format-independent OSNR monitoring insensitive to cascaded filtering effects by low-cost coherent receptions and RF power measurements

Zhenhua Dong,[1,*] Kangping Zhong,[2] Xian Zhou,[2] Chao Lu,[2] Alan Pak Tao Lau,[1] Yanzhao Lu,[3] and Liangchuan Li[3]

[1]*Photonics Research Centre, Department of Electrical Engineering, The Hong Kong Polytechnic University, Hung Hom, Kowloon, Hong Kong*

[2]*Photonics Research Centre, Department of Electronic and Information Engineering, The Hong Kong Polytechnic University, Hung Hom, Kowloon, Hong Kong*

[3]*Network Research Department, Huawei Technologies, Shenzhen, 518129, China*

[*]*dong.keke@gmail.com*

Abstract: Optical signal-to-noise ratio (OSNR) monitoring is indispensable for ensuring robust and flexible optical networks that provide failure diagnosis, dynamic lightpath provisioning and modulation format adaptation. We propose and experimentally demonstrate a low-cost, modulation-format-independent OSNR monitoring scheme utilizing reduced-complexity coherent receptions, electrical filtering and radio frequency (RF) power measurements. By measuring the RF power of the coherently received baseband signals at three different frequency components, the proposed OSNR monitor is also insensitive to spectral narrowing induced by cascaded wavelength selective switches (WSSs). We experimentally demonstrate accurate data-format-transparent and filtering-effect-insensitive OSNR monitoring for 25-Gbaud dual-polarization (DP-) transmissions with QPSK, 16-QAM and 64-QAM signals over various distances with different amount of filtering effects by cascaded WSSs. We further characterize the influence of different system parameters, such as the bandwidth of the electrical low-pass filter, the laser frequency offset and laser linewidth on the accuracy of the proposed OSNR monitor. The robustness of the proposed OSNR monitoring scheme to fiber nonlinearities, calibration parameter mismatches and variations of WSS parameters are also investigated.

OCIS codes: (060.1660) Coherent communications; (060.2330) Fiber optics communications; (060.2360) Fiber optics links and subsystems.

References and links

1. A. P. T. Lau, Y. Gao, Q. Sui, D. Wang, Q. Zhuge, M. Morsy-Osman, M. Chagnon, X. Xu, C. Lu, and D. V. Plant, "Advanced DSP techniques enabling high spectral efficiency and flexible transmissions: toward elastic optical networks," IEEE Signal Process. Mag. **31**(2), 82–92 (2014).
2. Q. Sui, A. P. T. Lau, and C. Lu, "Fast and robust blind chromatic dispersion estimation using auto-correlation of signal power waveform for digital coherent systems," J. Lightwave Technol. **31**(2), 306–312 (2013).
3. S. J. Savory, "Digital coherent optical receivers: algorithms and subsystems," IEEE J. Sel. Top. Quantum Electron. **16**(5), 1164–1179 (2010).
4. D. J. Ives, B. C. Thomsen, R. Maher, and S. J. Savory, "Estimating OSNR of equalised QPSK signals," in *Proc. Eur. Conf. Exhib. Opt. Commun. (ECOC)*, Geneva, Switzerland, Sep. 2011, Paper Tu.6.A.6.
5. M. S. Faruk, Y. Mori, and K. Kikuchi, "In-Band estimation of optical signal-to-noise ratio from equalized signals in digital coherent receivers," IEEE Photonics J. **6**(1), 7800109 (2014).
6. C. Zhu, A. V. Tran, S. Chen, L. B. Du, C. C. Do, T. Anderson, A. J. Lowery, and E. Skafidas, "Statistical moments-based OSNR monitoring for coherent optical systems," Opt. Express **20**(16), 17711–17721 (2012).

#233392 - $15.00 USD Received 29 Jan 2015; revised 2 Jun 2015; accepted 4 Jun 2015; published 9 Jun 2015

7. Z. Dong, A. P. T. Lau, and C. Lu, "OSNR monitoring for QPSK and 16-QAM systems in presence of fiber nonlinearities for digital coherent receivers," Opt. Express **20**(17), 19520–19534 (2012).
8. Z. Dong, Q. Sui, A. P. T. Lau, K. Zhong, L. Li, Z. Li, and C. Lu, "Optical performance monitoring in DSP-based coherent optical systems," in *Proc. Opt. Fiber Commun. (OFC),* Los Angeles, CA, Mar. 2015, Paper W4D.1.
9. C. C. Do, C. Zhu, and A. V. Tran, "Data-aided OSNR estimation using low-bandwidth coherent receivers," IEEE Photon. Technol. Lett. **26**(13), 1291–1294 (2014).
10. X. Liu, Y. H. Kao, S. Chandrasekhar, I. Kang, S. Cabot, and L. L. Buhl, "OSNR monitoring method for OOK and DPSK based on optical delay interferometer," IEEE Photon. Technol. Lett. **19**(15), 1172–1174 (2007).
11. S. Oda, J. Y. Yang, Y. Akasaka, K. Sone, Y. Aoki, M. Sekiya, and J. C. Rasmussen, "In-band OSNR monitor using an optical bandpass filter and optical power measurements for superchannel signals," in *Proc. Eur. Conf. Exhib. Opt. Commun. (ECOC)*, London, U. K., Sep. 2013, paper P.3.12.
12. G. Nakagawa, S. Oda, K. Sone, Y. Aoki, T. Hoshida, and J. C. Rasmussen, "Demonstration of integrated optical path monitoring sub-system in CDCG-ROADM network," in *2014 European Conference on Optical Communication* (IEEE, 2014), P.4.1.
13. C. Pulikkaseril, L. A. Stewart, M. A. Roelens, G. W. Baxter, S. Poole, and S. Frisken, "Spectral modeling of channel band shapes in wavelength selective switches," Opt. Express **19**(9), 8458–8470 (2011).
14. Optical Monitoring for DWDM Systems. ITU-T recommendation G.697, June 2004.
15. H. Rosenfeldt, I. Clarke, S. Frisken, G. Dash, X. Huang, H. Li, W. Cui, J. Zhang, J. Chen, Z. Kong, and S. Poole, "Miniaturized heterodyne channel monitor with tone detection," in *Optical Fiber Communication Conference*, OSA Technical Digest (online) (Optical Society of America, 2015), paper W4D.7.
16. VPIsystems™, "VPItransmission Maker™".
17. Y. Sakamaki, T. Kawai, T. Komukai, M. Fukutoku, and T. Kataoka, "Evaluation of optical filtering penalty in digital coherent detection system," IEICE Commun. Express **1**(2), 54–59 (2012).

1. Introduction

Fiber-optic communication networks are evolving to employ adaptive modulation formats and reconfigurable optical add/drop multiplexers (ROADMs) to enable flexibility, dynamicity and better utilization of available transmission capacity [1]. Optical performance monitors (OPM) are indispensable for such complex networks as they can provide failure diagnosis, optimization and real-time performance monitoring for dynamic lightpath provisioning and modulation format adaptation. Since linear impairments such as chromatic dispersion (CD) and polarization-mode dispersion (PMD) can be estimated [2] and compensated by numerous DSP algorithms [3], system performance is largely determined by the OSNR of received signals. So far, in-band OSNR monitoring can be easily realized at the receiver from the statistical moments or the distributions of equalized signals by relatively simple algorithms [4–7] and such OPM functionality is essentially a by-product of the digital coherent receiver. However, OSNR monitors need to be deployed ubiquitously across the network including intermediate nodes where coherent receiver solutions are simply too costly and impractical [8]. Consequently, a reliable, low-cost, modulation-format-independent OSNR monitor for distributed monitoring of optical networks is in demand. In [9], a data-aided OSNR estimation technique utilizes Golay sequences as its training symbols and obtains the OSNR from the variance of the power spectrum of Golay sequences as it is proportional to the expected value of noise power spectral density. The method only utilizes a low-bandwidth coherent receiver working at low sampling rate and is modulation-format-independent but requires the modification of transmitters. Another monitoring technique [10] proposed the use of an optical delay interferometer (ODI), by measuring the optical power of the constructive and destructive output ports using simple, low-speed photodiodes, to determine the power associated with the signal and the noise and thus determine the OSNR. However, the impact of spectral narrowing by cascaded WSSs limits the monitoring accuracy because the spectral shape needs to be constant along transmission. Recently, an OSNR monitoring method using tunable optical band pass filter with optical power measurements was reported in [11, 12]. However, the monitoring accuracy relies on the bandwidth of the optical filter and a very narrow bandwidth (several GHz, expensive and not commercially available at present) is needed to guarantee a good monitoring accuracy [11]. Besides, it may also suffer from WSS induced spectral narrowing.

#233392 - $15.00 USD Received 29 Jan 2015; revised 2 Jun 2015; accepted 4 Jun 2015; published 9 Jun 2015

In this paper, we propose a modulation-format-independent and low-cost OSNR monitor utilizing reduced-complexity coherent receptions, electrical filtering and RF power measurements. By measuring the RF power of three different frequency components of the coherently received baseband signals, the proposed technique is also insensitive to spectral narrowing by WSSs. We experimentally demonstrate accurate (<0.7 dB error) OSNR monitoring for various modulation formats and transmission distances, hence different number of WSSs. We also study the robustness of the proposed technique to the fiber nonlinearity, laser effects in a five-channel WDM system at 50-GHz spacing and other practical considerations.

2. Principle of proposed in-band OSNR monitor

Figure 1(a) shows the schematic diagram of the proposed in-band OSNR monitor as the key function of an OPM that can be deployed in different locations across an optical network. It consists of a tunable laser that functions as a local oscillator (LO), a 3dB coupler, a low-speed balanced detector (several GHz), a low-pass electrical filter, an RF power meter and a control and process unit (CPU). The incoming optical signals tapped from the transmission link firstly go into a 3dB coupler, where the signals interfered with the light of tunable laser. Since no phase or polarization information is required for the monitoring, a 3 dB coupler rather than a polarization diversity optical quadrature front-end (2 × 4 90° hybrid) is used to coherently receive the signals. After balance detection, the resulting baseband RF signals then go into an electrical low-pass filter. By tuning the frequency of the tunable laser to the center frequency f_{CF} and an offset frequency f_{OF1} of the target optical signal, the signal components around f_{CF} and f_{OF1} falls into the passband of the electrical filter and are measured by the RF power meter as P_{CF} and P_{OF1} respectively (See Fig. 1(b)). Here the tunable laser does not only act as a frequency selector, but, as an additional advantage, amplify the signal to a proper level to avoid the detrimental effects of electronic thermal noise on the accuracy of the proposed OSNR monitoring technique. Also it should be noted that the devices used in our proposed monitor such as the 3dB coupler, the tunable laser with a linwidth of few MHz, balanced detector with several GHz bandwidth and the electrical low-pass filter are all commercially available and low-cost.

In coherent receivers, for sufficiently high LO powers, ASE noise is usually dominant and other noise components like shot-noise and thermal noise can be neglected. Since the ASE noise can be modeled as additive white Gaussian noise (AWGN), its power P_{ASE} around frequencies f_{CF} and f_{OF1} within a given band are assumed to be the same, while the signal power P_{SIG} within the two bands are determined by the signal pulse shape which normally are not the same. The relationship between P_{CF}, P_{OF1}, P_{SIG} and P_{ASE} can be described as [11]

$$P_{CF} = P_{SIG} + P_{ASE}, \qquad P_{OF1} = R_1 P_{SIG} + P_{ASE}. \tag{1}$$

The calibration parameter R_1 can be obtained by placing the monitor at the transmitter (Tx) side and performing a back-to-back measurement where the ASE noise is negligible, i.e. $R_1 = P_{OF1\text{-}Tx}/P_{CF\text{-}Tx}$. The OSNR can then be calculated by the CPU as

$$OSNR = \gamma \frac{P_{SIG}}{P_{ASE}} = \gamma \frac{1 - P_{CF}/P_{OF1}}{(P_{CF}/P_{OF1})R_1 - 1}, \tag{2}$$

where the calibration parameter γ is determined by the electrical filter bandwidth and signal bandwidth.

#233392 - $15.00 USD Received 29 Jan 2015; revised 2 Jun 2015; accepted 4 Jun 2015; published 9 Jun 2015

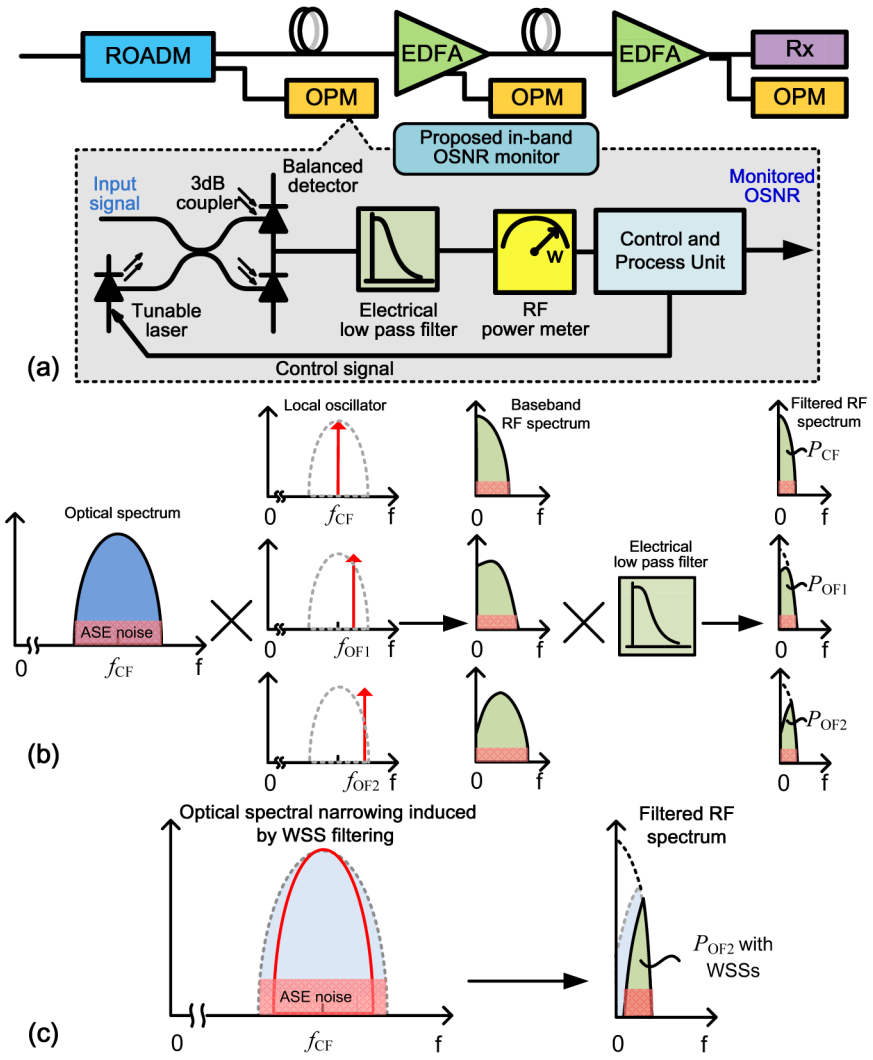

Fig. 1. (a) Schematic diagram of proposed OSNR monitor; (b) Signal spectra before and after coherent receptions; RF spectrum after electrical filtering showing filtered signal (marked in green) and ASE noise (marked in red), whereas P_{CF}, P_{OF1} and P_{OF2} denote RF power after electrical filtering when the LO frequency is set to the center frequency of the spectrum f_{CF} and two other offset frequencies f_{OF1} and f_{OF2}, (c) WSS filtering induced optical spectral narrowing and RF spectral narrowing. ROADM: reconfigurable optical add-drop multiplexer, EDFA: erbium-doped fiber amplifier, OPM: optical performance monitor, Rx: receiver. ASE: amplified spontaneous emission.

It should be noted that the calibration parameter R_1 depends on the signal spectral shape and remain unchanged only when there is no additional filtering effect. However, WSSs in ROADMs are essential parts of present optical networks and cascaded filtering effects by WSSs during signal transmission are known to affect spectral shapes. Figure 1(c) shows the spectral narrowing effect for a 25-Gbaud signal by cascaded WSSs. The shape of the sideband is obviously changed and thus the relationship in Eq. (1) will no longer hold which may lead to unacceptable OSNR monitoring errors. In order to cope with spectral narrowing in the OSNR monitoring, we can take another RF power measurement P_{OF2} at a second offset frequency f_{OF2} (See Fig. 1(b)) and define a calibration parameter R_2 similar to R_1. Additionally, two more parameters a and b are defined to characterize the effect of a WSS on

#233392 - $15.00 USD Received 29 Jan 2015; revised 2 Jun 2015; accepted 4 Jun 2015; published 9 Jun 2015

the spectral shape at f_{OF1} and f_{OF2} respectively, which can be obtained by placing a WSS between the transmitter and the monitor and performing a back-to-back measurement, or by verified theoretical models of WSS filter shapes [13]. In the presence of N cascaded WSSs in the transmission link, the measured power can be re-written as

$$P_{CF} = P_{SIG} + P_{ASE}, \qquad P_{OF1} = R_1 \alpha^N P_{SIG} + P_{ASE}, \qquad P_{OF2} = R_2 \beta^N P_{SIG} + P_{ASE}. \tag{3}$$

By solving the three equations above, we can obtain N, P_{SIG} and P_{ASE} and thus calculate the OSNR by the implicit equation

$$\frac{P_{OF1}}{P_{CF} R_1} + \frac{P_{OF1}/P_{CF} - 1}{R_1 \cdot OSNR} = \left(\frac{P_{OF2}}{P_{CF} R_2} + \frac{P_{OF2}/P_{CF} - 1}{R_2 \cdot OSNR} \right)^{\log \alpha / \log \beta}. \tag{4}$$

3. Experimental and simulation results

3.1 Experimental setup and results

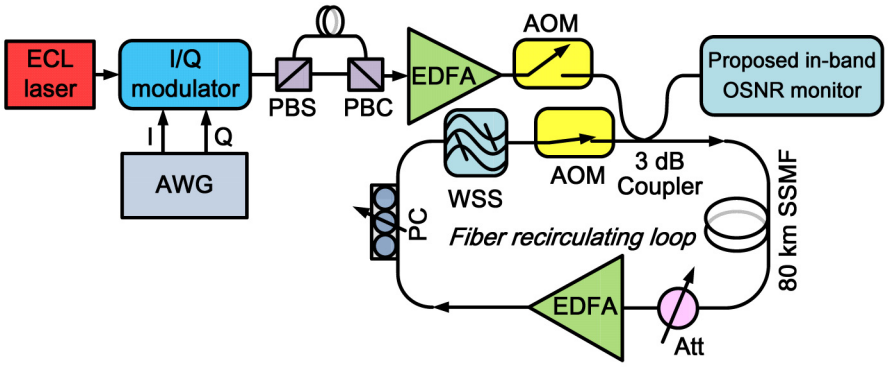

Fig. 2. Experimental setup. Att: attenuator, AWG: arbitrary waveform generator, AOM: acousto-optic modulator, ECL: external cavity laser, PBS: polarization beam splitter, PBC: polarizing beam combiner, PC: polarization controller, SSMF: standard single-mode fiber.

Figure 2 shows the experimental setup used to evaluate the performance of the proposed monitoring technique. At the transmitter side, an external cavity laser (ECL) sends a continuous-wave (CW) light with 100 kHz linewidth at 1553.12 nm and is modulated using an I/Q modulator, of which the I and Q branches are driven independently by two uncorrelated 25-Gbaud pseudo-random bit sequences (PRBSs) (length = 2^{15}-1) produced by the arbitrary waveform generator (AWG). In order to verify the transparence of the proposed technique to various modulation formats, we generate three common signals, DP-QPSK, DP-16-QAM and DP-64-QAM, by modulate the I/Q modulator with 2-level, 4-level and 8-level pulse-amplitude modulation (PAM) electrical signals, respectively. Polarization division multiplexing is achieved by splitting the signal through a polarization beam splitter (PBS) into two branches, delaying one branch, and recombining the signal through a polarization beam combiner (PBC). The signal is then amplified to around 0 dBm and launched into a fiber recirculating loop, which consists of a span of 80 km standard single-mode fiber (SSMF), an erbium-doped fiber amplifier (EDFA) and a programmable WSS. The EDFA fully compensates the total loss in the loop. A tunable attenuator is placed before the EDFA to realize various OSNR values for the received signals. The WSS is set to 50-GHz bandwidth with 5th-order super-Gaussian shape and with an all-pass shape for the two neighbouring channels as shown in Fig. 3. As a result, the out-band noise is preserved in the neighbouring channels even through the signal undergo cascaded filtering effects. At the loop output, the OSNR values of the received signals are measured by the proposed monitor which are then compared with the reference OSNR measured by an OSA using out-of-band noise

#233392 - $15.00 USD Received 29 Jan 2015; revised 2 Jun 2015; accepted 4 Jun 2015; published 9 Jun 2015

measurement [14] referring to 0.1 nm noise bandwidth. The RF power meter used in the experiments has a sensitivity of as low as −60 dBm and a frequency range from 10 MHz to 18 GHz. However, since the power meter cannot be triggered fast enough to measure the signals coming from the recirculating loop, we only use it to perform the back to back experiment. For those transmission experiments requiring fiber recirculating loop, a 80-Gsamples/s real-time oscilloscope is used instead of the RF power meter to measure the RF signal powers in the following steps: 1) Capturing a sequence (length = 400000) of the signals from the balanced detector, 2) filtering the signals with a digital low pass filter and 3) calculating the power of the signals. We again note that such real-time scope for RF power measurement is not required in realistic optical networks with straight-line links.

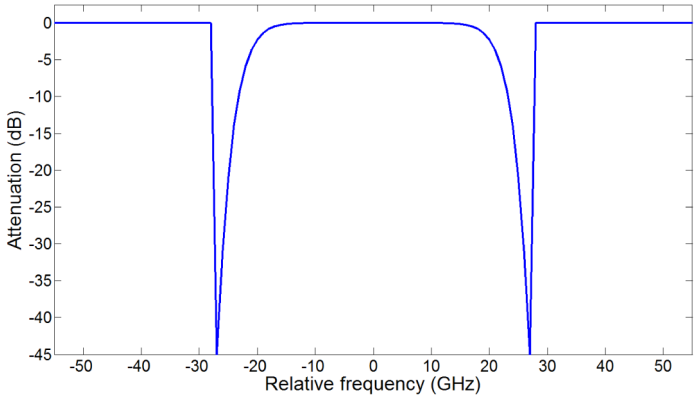

Fig. 3. Amplitude spectrum of the programmable WSS with 5th-order super-Gaussian transfer function for the channel of interest and all-pass shapes for the two neighboring channels.

The design parameters for the OSNR monitor include the bandwidth of the electrical low-pass filter and the offset frequency f_{OF1} and f_{OF2}, which determine the proposed monitoring accuracy [11]. Figure 4 shows the experimental results for the accuracy of the OSNR monitor of DP-64-QAM signals transmitted over 640 km by changing the bandwidth of the digital low-pass filter from 500 MHz to 8 GHz, whereas the f_{OF1} and f_{OF2} are fixed at f_{CF} + 20 GHz and f_{CF} + 23.5 GHz respectively. As expected, the filter with lowest bandwidth (500 MHz) resulted in the minimum error which is less than 0.2 dB, and the error level increases as the bandwidth increases. The maximum error will be larger than 1dB when the bandwidth is set to be larger than 6 GHz. Since a negligible error level increment of 0.1 dB occurs when the bandwidth increases from 500 MHz to 800 MHz, we choose the bandwidth of the low-pass filter to be 800 MHz for the rest of the paper so as to relax the sensitivity requirement of the RF power meter.

#233392 - $15.00 USD Received 29 Jan 2015; revised 2 Jun 2015; accepted 4 Jun 2015; published 9 Jun 2015

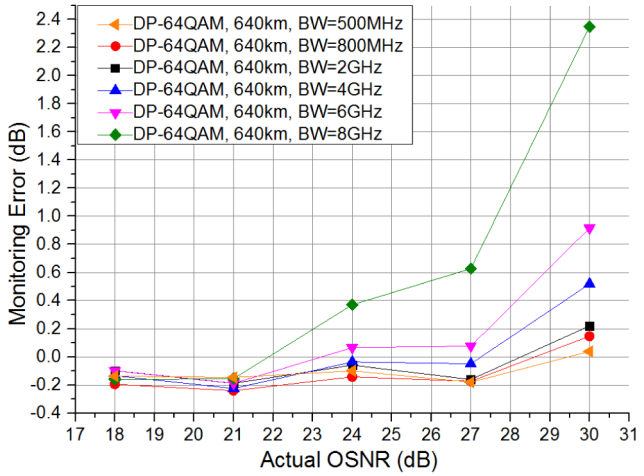

Fig. 4. Experimental OSNR monitoring error versus actual OSNR for DP-64-QAM signals transmitted over 640 km using an electrical filter with bandwidth from 500 MHz to 8GHz.

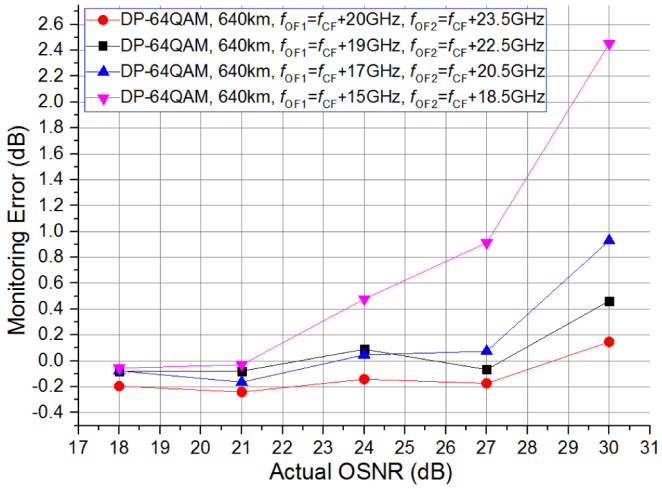

Fig. 5. Experimental OSNR monitoring error versus actual OSNR for DP-64-QAM signals transmitted over 640 km using various sets of offset frequency f_{OF1} and f_{OF2}.

Figure 5 shows the accuracy of the proposed OSNR monitoring scheme for DP-64-QAM signals transmitted over 640 km at different sets of f_{OF1} and f_{OF2}, whereas the frequency difference between f_{OF1} and f_{OF2} is fixed at 3.5 GHz. As shown, an error of larger than 1 dB occurs when the f_{OF1} and f_{OF2} are set at f_{CF} + 15 GHz and f_{CF} + 18.5 GHz respectively. As the offset frequencies are set closer to the edge of the signal spectrum, the error level decreases and a minimum error level of <0.3 dB is achieved by setting f_{OF1} and f_{OF2} at f_{CF} + 20 GHz and f_{CF} + 23.5 GHz respectively. We shall not further set f_{OF1} and f_{OF2} closer to the edge of the spectrum since in a WDM system overlaps of the neighboring channels may occur and a proper guard band (i.e., >1.5 GHz) between f_{OF2} and the edge frequency should be guaranteed.

In order to demonstrate the data-format independence and the insensitivity to filtering effects of the proposed monitor, we perform experiments for different modulation formats and different distance, i.e. different number of WSSs. To achieve best monitoring accuracy, we choose the electrical filter with a bandwidth of 800 MHz and set the offset frequencies f_{OF1} and f_{OF2} to be 20 GHz and 23.5 GHz respectively. It should be noted that we replace the digital low-pass filter by an analog filter to realize the experimental setup in a more practical

#233392 - $15.00 USD Received 29 Jan 2015; revised 2 Jun 2015; accepted 4 Jun 2015; published 9 Jun 2015

way. For DP-QPSK and DP-16-QAM signals, experiments of 640 km and 1280 km transmission are performed. For DP-64-QAM signal, experiments of back-to-back (BTB), 320 km and 640 km transmission are performed. We use the same sets of calibration parameters R_1, R_2, a and b determined by taking a back-to-back measurement using DP-16-QAM signals for all the OSNR calculations of different modulation formats and transmission distances. Each monitoring error is taken from the average of 8 independent measurements.

As shown in Fig. 6, for DP-64-QAM signals, the OSNR monitor achieved <0.6 dB accuracy for OSNR values from 18 to 30 dB and a transmission distance up to 640 km (8 WSSs), whereas for DP-16-QAM and DP-QPSK signals, monitoring error is less than 0.7 dB for OSNR values from 12 to 27 dB and a transmission distance up to 1280 km (16 WSSs). The accuracy of the monitoring results across different modulation formats and distances show that the OSNR monitor can perform accurately independent of the data format and insensitive to the WSS filtering. On the other hand, note that if we only use Eq. (2) to calculate the OSNR for DP-64-QAM signals after 640 km transmission i.e. 8 cascaded WSS filters, the maximum monitoring error can be larger than 5 dB (represented by the pink curve in Fig. 6). Therefore, incorporating P_{OF2} and some prior knowledge of the WSS filter shape in the OSNR monitoring is pivotal to its robustness against cascaded filtering effects.

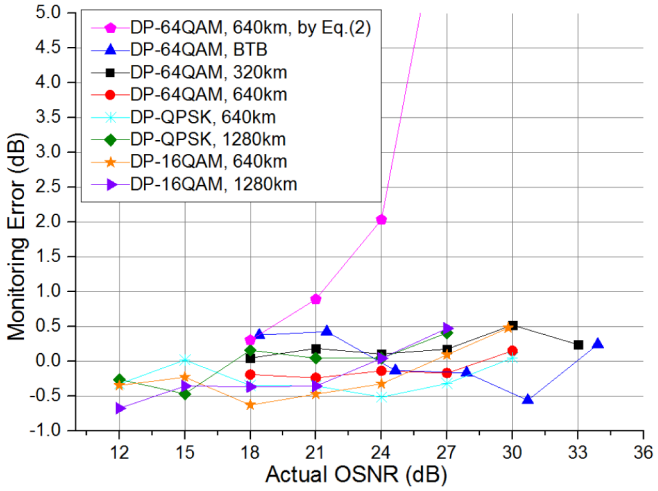

Fig. 6. Experimental OSNR monitoring error versus actual OSNR for DP-QPSK/16-QAM /64-QAM signals over various transmission distances (different number of WSSs). All the monitoring errors are less than 0.7 dB by using Eq. (4). The results showed in pink curve are the monitoring errors for DP-64-QAM signals after 640 km transmission obtained by using Eq. (2) when WSS filtering is not taken into account.

Since no frequency-locked loop (FLL) is used in the proposed monitor, frequency offset (FO) between the transmitter and receiver lasers will exist in practical applications. Figure 7 shows the OSNR monitoring errors for DP-64-QAM signals transmitted over 640 km with various amounts of intentionally introduced FO. As shown in the figure, the monitoring error increases with FO but a <0.9 dB monitoring error for FO up to 1 GHz for OSNR below 30 dB can still be maintained. Recently, a low-cost, fast-tuning MGY semiconductor laser co-packaged with a frequency-referencing etalon with < 0.5 GHz accuracy was demonstrated in [15] and can be used in our proposed monitor for accurate frequency tracking. Alternatively, one can identify the frequency that gives the largest P_{CF} in the electrical spectrum as the center frequency f_{CF} and carry out the calculations in Eq. (4). In that case, the absolute frequency offsets are no longer a detrimental factor and the monitoring accuracy are more robust to laser frequency offsets.

#233392 - $15.00 USD Received 29 Jan 2015; revised 2 Jun 2015; accepted 4 Jun 2015; published 9 Jun 2015

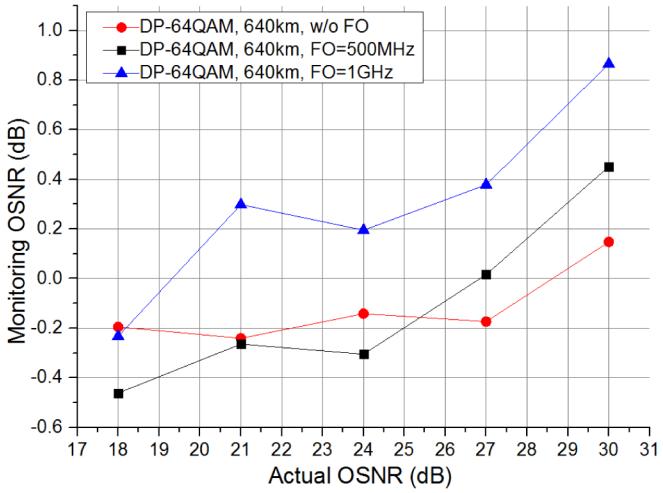

Fig. 7. Experimental OSNR monitoring error versus actual OSNR for DP-64-QAM signals transmitted over 640 km in the presence of different frequency offsets up to 1 GHz between the lasers of transmitter and receiver.

3.2 Robustness of the proposed OSNR monitoring technique to fiber nonlinearities, laser effects in WDM systems and other practical considerations

We conduct simulations using VPI [16] to investigate the influence of nonlinear effects in a WDM system on the accuracy of the proposed OSNR monitor. We perform WDM transmissions using five-channel 25-Gbaud DP-16-QAM and DP-64-QAM signals with 50-GHz channel spacing over 640 km fiber. The wavelength multiplexer at the transmitter end has 50-GHz bandwidth with 4th-order super-Gaussian shape. The remaining part of the system setup is the same as that shown in Fig. 2 and the bandwidth of the electrical filter, the offset frequencies f_{OF1} and f_{OF2} are chosen to be 800 MHz, 20 GHz and 23.5 GHz respectively, the same as those in the experiments.

Figure 8 shows the measured OSNR versus the actual OSNR for the DP-16-QAM and DP-64-QAM signals at 0 dBm and 4 dBm launched power per channel at the center channel (CH3) and at the edge channel (CH1) of a five-channel WDM system with 50-GHz ITU grid. In the presence of weak nonlinearities (0 dBm/channel), for OSNR values of <30 dB, the OSNR monitor achieves <0.4 dB accuracy for both the edge channel and the center channel for both modulation formats. The monitoring error of the edge channel CH1 is a little bit larger than that of center channel CH3 as the calibration parameters R_1, R_2, a and b used for the OSNR calculation of CH1 are obtained from CH3 and the true calibration parameters may slightly vary among different channels. However, the similarity of the depicted curves for different WDM channels verifies the wavelength independency of the proposed monitoring technique. As the launched power increases to 4 dBm per channel, some nonlinearity is present and the monitoring accuracy is reduced due to the nonlinearity-induced spectrum broadening. It can be seen that the monitoring accuracy of center channel suffers more nonlinearities than the edge channel since the center channel is more vulnerable to cross phase modulation effects. However, the error levels of both channels and both modulation formats are still less than 1 dB which indicate that the proposed method can work properly in the presence of moderate amount of nonlinearity.

#233392 - $15.00 USD Received 29 Jan 2015; revised 2 Jun 2015; accepted 4 Jun 2015; published 9 Jun 2015

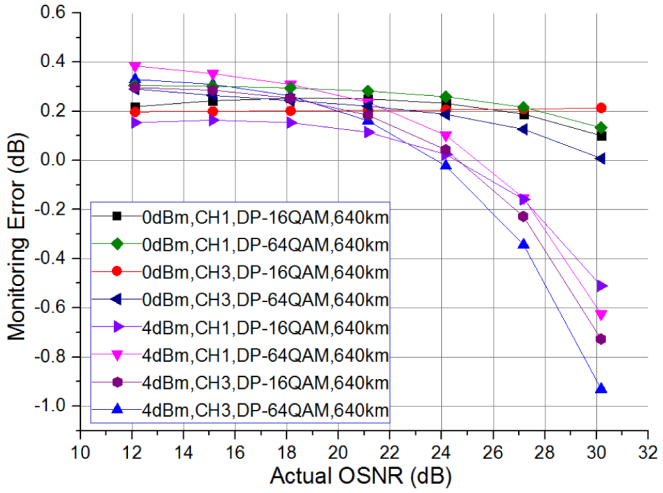

Fig. 8. Simulated OSNR monitoring error versus actual OSNR for DP-16-QAM and DP-64-QAM signals transmitted over 640 km of different channels in a WDM system at different launched power per channel.

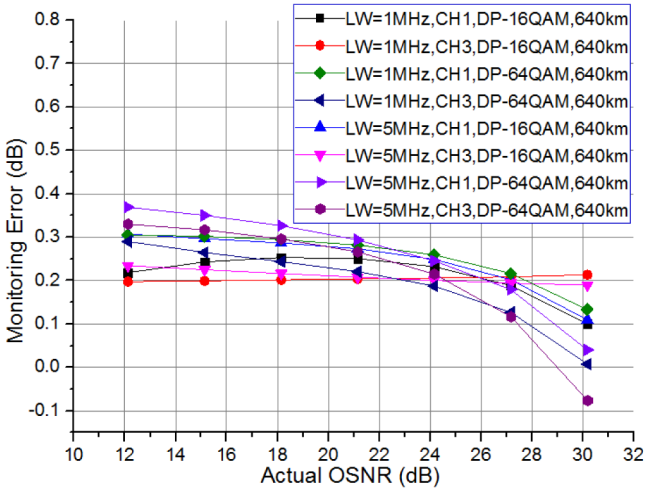

Fig. 9. Simulated OSNR monitoring error versus actual OSNR for DP-16-QAM and DP-64-QAM signals transmitted over 640 km of different channels in a WDM system using LO with 1-MHz and 5-MHz linewidth.

We also investigate the influence of the linewidth of the tunable laser on the accuracy of the proposed OSNR monitor in the WDM system. In order to realize the monitor in a low-cost fashion, the tunable laser used inside the monitor as the LO is preferred to be realized by a DFB laser with a typical linewidth (LW) of several MHz. Figure 9 compares the performance of the OSNR monitor using the LO with a linewidth of 1 MHz and 5 MHz for DP-16-QAM and DP-64-QAM signals of both edge channel and center channel. It can be seen from the figure that the error levels increase only very slightly with the linewidth of both channels and modulation formats. The maximum error increases by 0.2 dB as the linewidth increases from 1 MHz to 5 MHz and the maximum error of both channels and modulation formats are still less than 0.4 dB.

In addition, the calibration parameters R_1, R_2, a and b used for all the OSNR calculations are determined by taking a back-to-back measurement using DP-16-QAM signals at the center channel. It should be noted that R_1, R_2 depends on the signal spectral shape and α, β

#233392 - $15.00 USD Received 29 Jan 2015; revised 2 Jun 2015; accepted 4 Jun 2015; published 9 Jun 2015

depends on the WSS shape at f_{OF1} and f_{OF2} and these calibration parameters may vary with the constituent devices in practice, which in turn may affect the OSNR monitoring accuracy. We performed simulations to monitor the OSNR of received DP-QPSK signals after 800 km transmission through 10 WSSs to investigate the impact of the calibration parameters mismatch on the monitoring error and the results are shown in Fig. 10. When these 4 parameters are off by less than 8% of their actual values, the monitoring errors can still be kept under 1 dB. On the other hand, note that the estimated number of cascaded WSSs N (shown in the legend), deviates from its actual value 10 considerably. Fortunately, that is of little concern for our overall objective of accurate OSNR monitoring.

Further to calibration parameter mismatches, the center frequencies, bandwidths and even the shapes of WSS may vary slightly from channel to channel and from device to device in practice, which in turn can affect the accuracy of the proposed OSNR monitoring scheme. We performed simulations for DP-QPSK transmissions over 800 km with non-identical WSSs and the results are shown in Fig. 11. The 10 WSSs are assigned with different center frequency, bandwidth and the order of super-Gaussian shape. In case 1, all the 10 WSSs are identical and well-aligned without any frequency shift. The bandwidth and order of super-Gaussian function of each WSS are 50 GHz and 4, respectively. In the 'interleaved' case 2 and case 3 [17], the center frequency shift is –2 and –3 GHz for about half the WSSs and + 2 and + 3 GHz for the remaining WSSs, respectively. In the 'unidirectional' case 4 and case 5, all the WSSs have the same center frequency shift of + 3 and –3 GHz, respectively. In the case 6 and case 7, all the WSSs have the same bandwidth of 47 GHz and 53 GHz, respectively. In the case 8 and case 9, all the WSSs have the same 3rd-order super-Gaussian shape and 5th-order super-Gaussian shape, respectively. In the case number 10, all the 10 WSSs are not identical and are randomly picked from cases 1-9. As can be seen from Fig. 11, the estimated N (shown in the legend with N = 10 as correct value) is very sensitive to such WSS parameter variations. For the OSNR estimates, the worst case scenario occurs when all the WSSs have a + 3 GHz frequency shift (case 4) and the largest error is nearly 0.9 dB i.e. a <1 dB monitoring error can be obtained when the cascaded WSSs are not identical. It seems that the overall effect of spectrum narrowing of cascaded WSSs with different center frequencies, bandwidths and shapes will mostly affect the accuracy of the estimated number of WSS N while the accuracy of the estimated OSNR is less sensitive to such variations and perturbations.

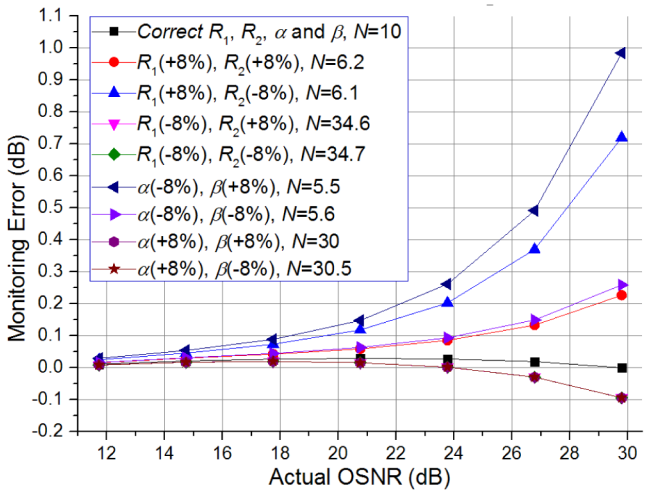

Fig. 10. Simulated OSNR monitoring error versus actual OSNR for DP-QPSK signals transmitted over 800 km under different degrees of calibration parameter mismatches.

#233392 - $15.00 USD Received 29 Jan 2015; revised 2 Jun 2015; accepted 4 Jun 2015; published 9 Jun 2015

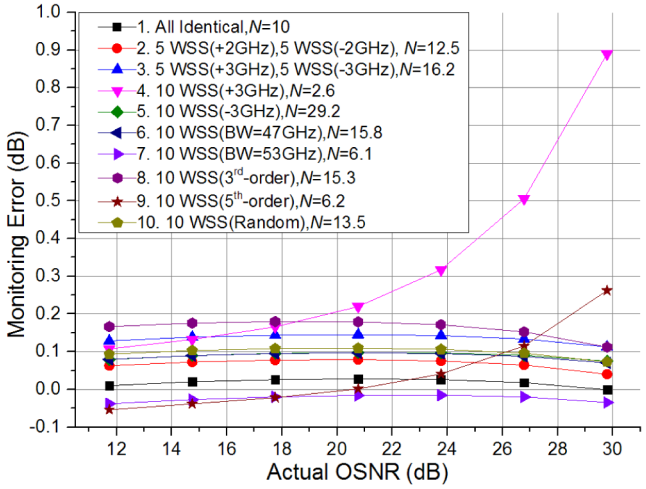

Fig. 11. OSNR monitoring error versus actual OSNR for DP-QPSK signals transmitted over 800 km with non-identical cascaded WSSs.

4. Conclusions

In this paper, we proposed and demonstrated a low-cost, modulation-format-independent OSNR monitoring scheme using a low-cost and reduced-complexity coherent receiver, simple electrical filtering and RF power measurements. By measuring and processing the RF power of three different frequency components of the coherently received baseband signals, the proposed OSNR monitor is also insensitive to spectral narrowing effects induced by cascaded WSSs. We experimentally studied OSNR monitoring for 25-Gbaud DP-QPSK, DP-16-QAM and DP-64-QAM signals transmitted over various distance (hence different number of WSSs) and demonstrated accurate OSNR monitoring across a wide range of system conditions. In addition, we investigated the influence of different parameters, including the bandwidth of the electrical low-pass filter, the laser frequency offset and laser linewidth on the monitoring accuracy. The proposed technique is also shown to be robust to the fiber nonlinearities, calibration parameter mismatches and random variations of WSS parameters within a certain range.

Acknowledgments

The authors would like to acknowledge the support of the Hong Kong Government General Research Fund under project number PolyU 152079/14E.

#233392 - $15.00 USD Received 29 Jan 2015; revised 2 Jun 2015; accepted 4 Jun 2015; published 9 Jun 2015